VLBA Continuum Observations of NGC 4258: Constraints on an Advection-Dominated Accretion Flow

J. R. Herrnstein[1], L. J. Greenhill[2], J. M. Moran[2], P. J. Diamond[1], M. Inoue[3], N. Nakai[3], and M. Miyoshi[4],

ABSTRACT

We report a 3σ upper limit of $220\,\mu$Jy on any 22-GHz continuum emission coincident with the central engine in NGC 4258. If NGC 4258 is powered by an advection-dominated accretion flow, this radio upper limit implies that the inner advection-dominated flow cannot extend significantly beyond $\sim 10^2$ Schwarzschild radii.

Subject headings: accretion, accretion disks — galaxies: active — galaxies: nuclei — galaxies: individual (NGC 4258) — masers

1. Introduction

NGC 4258 is a weakly active Seyfert 2 galaxy possessing a highly obscured central X-ray source with a 2–10 keV luminosity of 4×10^{40} erg s^{-1} (Makishima *et al.* 1994) and nuclear continuum and narrow line emission seen in reflected, polarized optical light (Wilkes *et al.* 1995). The galaxy also harbors one of the first known nuclear megamasers (Claussen, Heiligman, & Lo 1984), and VLBA observations reveal a nearly edge-on, extremely thin, slightly warped Keplerian disk (Watson & Wallin 1994; Greenhill *et al.* 1995; Miyoshi *et al.* 1995; Moran *et al.* 1995; Herrnstein, Greenhill, & Moran 1996). The masers extend from 0.13 to 0.26 pc (for a distance of 6.4 Mpc), and the Keplerian rotation curve requires a central binding mass, M, of $3.5 \pm 0.1 \times 10^7$ M$_\odot$ within 0.13 pc. The velocity centroid

[1]National Radio Astronomy Observatory, PO Box O, Socorro, NM 87801

[2]Harvard-Smithsonian Center for Astrophysics, Mail Stop 42, 60 Garden Street, Cambridge, MA 02138

[3]Nobeyama Radio Observatory, National Astronomical Observatory, Minamimaki, Minamisaku, Nagano 384-13, Japan

[4]Mizusawa Astrogeodynamics Observatory, National Astronomical Observatory, 2-12 Hoshigaoka, Mizusawa Iwate 023, Japan

of the disk agrees well with the optically-determined systemic velocity of the galaxy, and the rotation axis of the disk is aligned with the inner portion of large-scale twisted jets seen in radio to X-ray emission (Cecil *et al.* 1992). VLBA continuum observations also reveal a subparsec-scale jet oriented along the disk axis (Herrnstein *et al.* 1997). The central mass estimate provided by the maser observations corresponds to an Eddington luminosity, L_E, of $4.4 \pm 0.1 \times 10^{45}\,\mathrm{erg\,s^{-1}}$. The bolometric luminosity, L, is more difficult to estimate because the central edge-on disk obscures the nuclear emission. Wilkes *et al.* (1995) estimate $L \sim 10^{42-44}\ \mathrm{erg\,s^{-1}}$ based on observations of the nuclear continuum in optical, polarized light. However, the 2–10 keV X-ray flux suggests $L \sim 4 \times 10^{41}\ \mathrm{erg\,s^{-1}}$, based on the argument that the X-ray luminosity typically accounts for $\sim 10\%$ of L in AGN (Mushotsky, Done, & Pounds 1993). Hence $L \sim 10^{42\pm1} = 10^{-3.6\pm1} L_E$, and the central source in NGC 4258 is highly sub-Eddington.

Between 0.13 and 0.26 pc (4×10^4 and 8×10^4 Schwarzschild radii, R_S), the masers appear to trace a cool, thin accretion disk: the temperature in the maser layer must be between approximately 300 and 1000 K to support maser action, and the aspect ratio of the layer is less than 0.3% (Moran *et al.* 1995). Unfortunately, the structure within 0.13 pc is not directly observable, and the precise nature of the NGC 4258 central engine remains obscure. One possibility is that the outer thin disk traced by the masers extends to the central black hole, and that the NGC 4258 central engine is fueled by an optically thick, geometrically thin accretion disk (Shakura & Sunyaev 1973). Since the radiative efficiency, η (defined through $L = \eta \dot{M} c^2$, where $\dot{M}$ is the accretion rate), of such a disk is high, the sub-Eddington luminosity of NGC 4258 then implies a correspondingly sub-Eddington $\dot{M}$. Specifically, for $\eta = 0.1$, $\dot{m} \equiv \dot{M}/\dot{M}_E = 10^{-3.6\pm1}$. Here $\dot{M}_E$ is the Eddington accretion rate, given by $2.2 \times 10^{-8} M\,\mathrm{M_\odot\,yr^{-1}}$. Neufeld & Maloney (1995) argue that for $\dot{m} \sim 10^{-4.0}\alpha$, the outer disk, which is obliquely irradiated by the central X-ray source as a result of the warp, changes from cool molecular gas to warm atomic gas at about 0.23 pc, providing a natural explanation for the observed outer edge to the maser emission. Here, α is the standard Shakura-Sunyaev parameterization of the kinematic viscosity. In the Neufeld & Maloney model, $\eta \sim 10^{-0.6\pm1}\alpha^{-1}$.

Alternatively, Lasota *et al.* (1996; hereafter L96) have proposed that NGC 4258 harbors an optically thin advection-dominated accretion flow (ADAF) at small radii, within the cool molecular disk. Narayan & Yi (1994, 1995a&b; hereafter NY95b) have demonstrated the stability and self-consistency of a geometrically thick, optically thin accretion flow in which an extremely hot ($T \sim 10^{12}\,\mathrm{K}$) ion plasma coexists with much cooler ($T \sim 10^{9.5}$ K) electrons. For the ions, the radiative timescale is much longer than the accretion timescale. Thus, in the case of accretion onto a black hole (BH), the majority of the viscously dissipated energy is carried through the event horizon of the BH by the hot ions,

and the ADAF radiative efficiency is several orders of magnitude less than that of the standard thin disk. The appeal of the two-temperature ADAF models is that the optically thin synchrotron, bremsstrahlung, and Compton emission from the $\sim 10^{9.5}$ K electrons can account for the spectra of a broad variety of accreting systems over many decades in energy (see Narayan 1997 for a recent review). For example, efforts to model the radio-to-γ-ray spectrum of the galactic source Sgr A* with an ADAF spectrum are reasonably successful (Narayan, Yi, & Mahadevan 1995; Manmoto, Mineshige, & Kusunose 1998; Narayan *et al.* 1998). This is an important result: optically thick, thin disk models emit largely as blackbodies and are generally too cool to account for the X-ray emission observed in accreting binaries and active galactic nuclei (AGN).

The two-temperature ADAF solution is valid for accretion rates less than $\dot{m}_c \sim 1.3\alpha^2$ (Esin *et al.* 1997) or, equivalently, for bolometric luminosities less than $\sim 1.3\alpha^2 L_E$. NGC 4258 satisfies this requirement for $\alpha > 10^{-1.9\pm0.5}$. In general, the ADAF models are parameterized in terms of M, α, $\dot{m}$, β (the ratio of gas pressure to total pressure), and r_{tr} (the transition radius from the outer thin disk to the inner ADAF). The NGC 4258 ADAF model of L96 is constrained primarily by the maser disk binding mass and the 2–10 keV X-ray luminosity and spectral index, and secondarily by the polarized optical flux. L96 assume $\beta = 0.95$ and find that an NGC 4258 ADAF requires $\dot{m} \sim 10^{-1.8}\alpha$. More recent calculations suggest $\dot{m} \sim 10^{-1.6}\alpha$ (Narayan, personal communication), and the condition $\dot{m} \lesssim \dot{m}_c$ requires $\alpha \gtrsim 0.02$ in NGC 4258. In this model, $\eta \sim 10^{-3\pm1}\alpha^{-1}$, and the NGC 4258 ADAF is very rapid, but very inefficient in producing radiation.

In general, the hot ADAF electrons are expected to generate significant radio emission via the thermal synchrotron process. Unfortunately, most of the underluminous AGN and quiescent ellipticals which plausibly harbor ADAFs also possess core-jet radio structures that are not directly associated with the ADAF itself. In practice it is extremely difficult to discriminate this emission from the ADAF synchrotron emission. Even when VLBI provides sufficient angular resolution to resolve individual components within the radio core, it is usually impossible to determine which, if any, of this emission originates precisely at the central engine, where the ADAF emission must arise. Because the relative position of the center of mass of the sub-parsec molecular disk can be measured to a fraction of a milliarcsecond with VLBI, NGC 4258 provides a rare opportunity to circumvent the ambiguity associated with core-jet emission, and to test the radio portion of the proposed ADAF spectrum directly.

2. Observations and Analysis

NGC 4258 was observed at 22 GHz on 1997 March 7, March 23, and April 7 for 12, 14, and 15 hours, respectively, with the VLBA, phased VLA, and 140-foot Green Bank telescope of the NRAO [5], and the 100-meter MPIfR telescope. Eight, 8-MHz bands were observed, two of which were dedicated to observing the systemic maser emission centered at 470 $\mathrm{km\,s^{-1}}$ (LSR, radio definition). The maser emission in NGC 4258 extends from $\sim -500\,\mathrm{km\,s^{-1}}$ to $1500\,\mathrm{km\,s^{-1}}$, and the remaining bands were positioned between 1707 and $2354\,\mathrm{km\,s^{-1}}$ and -738 and $-1386\,\mathrm{km\,s^{-1}}$ to provide continuum coverage devoid of maser emission. In each epoch, 14-minute scans of NGC 4258 were interleaved with 3-minute observations of a nearby delay and fringe-rate calibrator (either 1308+33 or 4C39.25). The VLA was phased prior to each scan with observations of either 1144+399 or 1308+33.

Calibration was performed in AIPS using standard techniques. Gross amplitude calibration was accomplished using recorded system temperatures and tabulated values for the antenna system equivalent flux densities at 22 GHz. Amplitude self-calibration was performed on a strong maser feature, and we estimate the absolute amplitude calibration to be accurate to about 10%, or about 0.2 mJy for the NGC 4258 continuum flux. This dominates the 0.1 mJy thermal noise in the continuum images. Phase self-calibration was performed on the strong maser at $492\,\mathrm{km\,s^{-1}}$ after correcting for any residual clock offsets and drifts, and the resulting phase corrections were applied to the entire dataset in order to stabilize the interferometer.

Figure 1 shows the weighted average of the images, as well as the best-fitting warped-disk model. The disk model, and in particular the disk center, is determined using a global χ^2 minimization code (Herrnstein 1997) in which the maser positions and line-of-sight (LOS) velocities are used to define the best-fitting warped-disk model, parameterized in terms of the disk center, the central mass, and two polynomials in radius describing the three-dimensional warp of the disk. Formal parameter uncertainties are estimated using a Monte Carlo analysis in which χ^2 minimizations are performed on an ensemble of model disks sampled consistently with the actual data. Herrnstein (1997) reports uncertainties in the fitted disk center of $30\,\mu$as ($= 1 \times 10^{-2}\,\mathrm{pc} = 3 \times 10^2\,\mathrm{R}_S$) and $50\,\mu$as ($= 2 \times 10^{-2}\,\mathrm{pc} = 5 \times 10^2\,\mathrm{R}_S$) in right ascension and declination, respectively.

The 22-GHz continuum emission traces a jet-like structure oriented along the rotation axis of the maser disk and comprised of distinct northern and southern components that are

[5]The National Radio Astronomy Observatory is operated by Associated Universities, Inc, under cooperative agreement with the National Science Foundation.

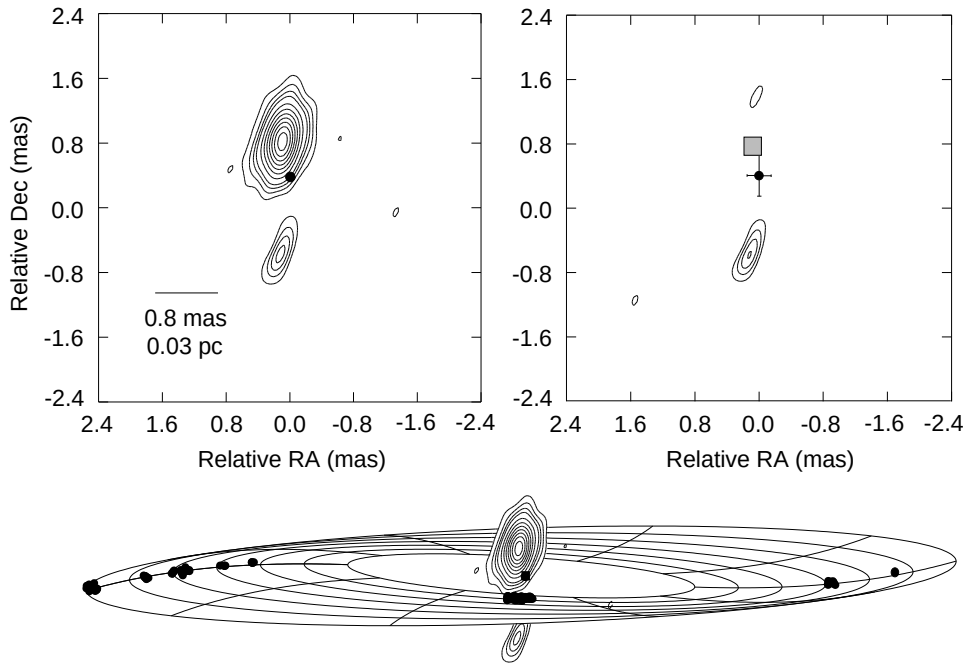

Fig. 1.— *Upper left:* 22-GHz VLBA continuum image of NGC 4258. Three, 14-hour observations have been combined in generating the image. The filled circle marks the center of mass of the maser disk. The thermal noise in the map is 72 μJy. *Upper right:* Continuum image after deconvolving the northern jet emission from the (u,v) dataset. The clean box used in the doconvolution is shown as a filled square. The disk center is marked with 5σ uncertainties. *Bottom:* The continuum map superposed on the best-fitting warped disk model. The masers are shown as filled circles, the disk center as the filled square.

each unresolved by the 0.6 by 0.3 mas beam. The flux density of the northern component varied from 2.5 to 3.5 ($\pm$0.3) mJy during the three epochs, while the southern component remained constant at 0.5 ± 0.1 mJy. These correspond to brightness temperature lower limits of 1×10^7 and 2×10^6 K for the northern and southern components, respectively. The centroid of the northern component appeared between 0.35 ± 0.02 mas and 0.46 ± 0.01 mas north of the disk center, while the southern feature remained stationary at -1.0 ± 0.06 mas. The new data are consistent with earlier studies of the NGC 4258 jet (Herrnstein *et al.* 1997). The ~ 0.4 mas (4×10^{16} cm or 4×10^3 R_S) offset of the northern jet emission from the disk center is highly significant compared to the ~ 0.05 mas statistical uncertainty, and can be explained by optical depth effects along a mildly relativistic jet (Blandford & Königl 1979; Herrnstein *et al.* 1997). The relative faintness of the southern jet is probably due to thermal free-free absorption in a thin surface layer of ionized gas along the near edge of the disk, which intercepts the LOS to the southern component. In this case, the relatively large offset of the southern source from the disk center occurs because the disk free-free opacity is approximately proportional to $1/r^2$, where r is the distance from the central X-ray source (Herrnstein, Greenhill, & Moran 1996).

We searched for continuum emission at the fitted-disk center of mass in each epoch by removing the northern jet emission from the (*u,v*)-data and re-imaging. This subtraction was accomplished by extracting from the (*u,v*)-data only that emission located within a $\sim 0.24 \times 0.24$ mas clean-box centered on the peak of the northern jet emission. In each epoch, this box lay north of the 5σ confidence interval for the disk center, and it is extremely unlikely that any central continuum emission has been inadvertently removed in the deconvolution process. There is no evidence for any central 22-GHz continuum emission within the 5σ interval around the disk center in any of the three epochs. Figure 1 shows the weighted average of the deconvolved images, together with the clean-box (for the second epoch) and the 5σ uncertainty in the position of the disk center. The map has a thermal noise of about 72 μJy, and *we report a 3σ upper limit of 220 μJy on any continuum emission coincident with the central mass of the NGC 4258 maser disk.* This corresponds to a brightness temperature lower limit of $8 \times 10^5 (r_a/5 \times 10^{16}\ \mathrm{cm})^{-2}$ K, where r_a is the (undetected) source size, in cm. The outer thin disk is tipped down from the LOS by $8 \pm 1^\circ$ at 0.13 mas, and, given the shape of the warp between 0.13 and 0.26 pc, it is unlikely that the thin molecular disk significantly obscures any central radio emission.

3. Discussion

The most direct method to discriminate between the standard thin-disk and ADAF accretion modes would be to determine the accretion rate through the outer thin disk. For a Shakura-Sunyaev accretion disk in hydrostatic equilibrium (c.f. Frank, King, & Raine 1992)

$$\frac{\dot{m}}{\alpha} \simeq 530 \frac{\mathrm{M}_D c_s^2}{M^{3/2}(r_2^{1/2} - r_1^{1/2})} \quad , \tag{1}$$

where M_D is the disk mass (in solar masses) between r_1 and r_2 (in pc), and c_s is the isothermal sound speed in $\mathrm{km\,s^{-1}}$. The observed upper limit in the thickness of the maser layer, together with the mere presence of the masers, implies $c_s \lesssim 2.5\,\mathrm{km\,s^{-1}}$ (or $T \lesssim 1000\mathrm{K}$) (Moran *et al.* 1995). The simplest assumption is that the masers lie in the midplane of the disk and that the midplane density must be less than $\sim 10^{10}\,\mathrm{cm^{-3}}$ to avoid thermal quenching of the population inversion. In this case, $\mathrm{M}_D \lesssim 5.8 \times 10^4\,\mathrm{M}_\odot$ between 0.13 and 0.26 pc and $\dot{m}/\alpha \lesssim 10^{-2.2}$. A second, more observationally motivated constraint on M_D comes from the precision of the Keplerian rotation curve of the high-velocity masers. While the statistical scatter in the LOS velocities around the best-fitting Keplerian rotation curve is about $3\,\mathrm{km\,s^{-1}}$, the systematic deviation from Keplerian rotation (δv) across the masing zone may be considerably larger due to uncertainties in the fitted-disk parameters, which are partially correlated. A formal χ^2 analysis demonstrates $\delta v \lesssim 20\,\mathrm{km\,s^{-1}}$. This requires $\mathrm{M}_D \lesssim 1.5 \times 10^6\,\mathrm{M}_\odot$ and $\dot{m}/\alpha \lesssim 10^{-0.8}$. This is about six times larger than the ADAF accretion rate. Thus, the maser data do not definitively rule out either mode of accretion in NGC 4258, and the present continuum observations provide an important additional constraint on the models.

We associate the center of the maser disk with the NGC 4258 central engine, and interpret the continuum non-detection in the context of the ADAF models using the analytical expressions presented in Mahadevan (1997; hereafter M97), which duplicate reasonably well the numerical results of NY95b. M97 includes all the relevant electron heating and cooling terms, but considers only the region between 3 and 10^3 R_S, assumes that the electron temperature, T_e, is constant and much less than the ion temperature over these radii, and treats the flow as purely spherical. These approximations are justified by the more detailed analysis of NY95b.

M97 treats the ADAF as a relativistic thermal plasma, which is valid for $\dot{m} \gtrsim 10^{-4}\alpha^2$ (Mahadevan & Quataert 1998) and is justified in NGC 4258. M97 shows that the radius, r_ν, at which the spherical flow becomes optically thick to synchrotron self-absorption depends on frequency, ν, as

$$r_\nu = 0.47 T_e^{8/5} \nu^{-4/5} M^{-2/5} \dot{m}^{3/5} \alpha^{-2/5}\ \mathrm{R}_S, \tag{2}$$

where we have assumed $\beta = 0.5$. To a very good approximation, the synchrotron spectrum, L_ν, is completely determined by the emission at r_ν, which may be approximated by a blackbody spectrum, B_ν, in the Rayleigh-Jeans limit (M97):

$$L_\nu = \pi B_\nu 4\pi r_\nu^2 = 2.3 \times 10^{-25} T_e^{21/5} \nu^{2/5} M^{6/5} \dot{m}^{6/5} \alpha^{-4/5} \text{ erg s}^{-1}. \quad (3)$$

Equations 2 and 3 show that both r_ν and L_ν are steep functions of the electron temperature. However, the analytical treatment of M97 and the more rigorous numerical work of NY95b both indicate that for high accretion-rate systems, the electron temperature is confined to a narrow range, and is essentially independent of the central mass. Specifically, M97 finds that for $\dot{m} \sim 10^{-1.5}\alpha$, $2.1 \times 10^9 \lesssim T_e \lesssim 3.1 \times 10^9$ over 9 decades in M.

For $\dot{m} = 10^{-1.6}\alpha$, $M = 3.5 \times 10^7\,\mathrm{M}_\odot$, and $T_e = 2.15 \times 10^9\,\mathrm{K}$, equation 3 indicates that $F_{22} \gtrsim 220\,\mu\mathrm{Jy}$ for $\alpha > 0.009$. Here F_{22} is the 22-GHz ADAF flux density assuming a distance of 6.4 Mpc. For $\alpha \lesssim 10^{-2}$, $\dot{m} \gtrsim \dot{m}_c$ and advection is not a viable solution. Hence, the ADAF models significantly overestimate the actual 22-GHz emission over the full range of allowed α. Here, we have assumed that r_{tr} is larger than the effective 22-GHz photosphere (r_{22}) as given by equation 2, a necessary prerequisite to the assumption of constant T_e. However, the absence of detectable 22-GHz continuum emission in NGC 4258 may be consistent with an ADAF that is truncated such that $r_{tr} < r_{22}$. Equation 2 indicates that $r_{22} \simeq 300\alpha^{1/5}\,\mathrm{R}_S$ for the NGC 4258 ADAF, suggesting that $r_{tr} \lesssim 10^2\,\mathrm{R}_S$ for typical values of α. A second, more stringent upper limit on r_{tr} comes from assuming that, for those frequencies below which the condition $r_\nu \gtrsim r_{tr}$ is satisfied, the emission follows the $T = 2.5 \times 10^9$ blackbody spectrum of the outermost ADAF shell at $r = r_{tr}$. In this case, the 22-GHz upper limit requires $r_{tr} \lesssim 80\,\mathrm{R}_S$. *Thus, the 220 μJy, 3σ upper limit on any compact 22-GHz emission coincident with the central engine in NGC 4258 implies that the proposed central ADAF cannot extend significantly beyond* $\sim 10^2\,R_S$. More rigorous numerical methods also lead to ADAF solutions consistent with the present 22-GHz upper limit for $r_{tr} \lesssim 10^2\,\mathrm{R}_S$ (Narayan, personal communication).

In addition to affecting the radio emission, the transition radius affects both the hard X-ray spectrum and the optical/UV emission. In the former case, the ADAF is Compton cooled by the soft photons from the outer cool disk, and as r_{tr} moves inward, the hard X-rays are suppressed. L96 find that $r_{tr} \gtrsim 10\,\mathrm{R}_S$ is consistent with the Makishima *et al.* (1994) measurements. The optical/UV spectrum depends on r_{tr} because the blackbody spectrum of the non-molecular portion of the disk peaks at these wavelengths. Wilkes *et al.* (1995) have measured the 5500 Å flux toward NGC 4258 in polarized light. This emission presumably arises in the central engine and has been scattered into our LOS. The corresponding 5500 Å central engine luminosity is highly sensitive to the type of scattering screen invoked (dust or electrons), and Wilkes *et al.* (1995) estimate that

$L_{5500} \sim 10^{37-39}\,\mathrm{erg\,s^{-1}\,\AA^{-1}}$. L96 find that the NGC 4258 ADAF contributes only about $10^{36.3}\,\mathrm{erg\,s^{-1}\,\AA^{-1}}$ at 5500 Å, and here we estimate the contribution of the thin disk to the 5500 Å luminosity for a range of r_{tr}.

The inferred isotropic luminosity of an optically thick, steady, thin disk truncated at r_{tr} is (c.f. Frank, King, & Raine 1992):

$$L_\lambda^{(td)} \simeq \frac{16\pi^2 h\nu^2 \cos i}{\lambda^3} \int_{r_{tr}}^{r_{out}} \frac{r dr}{e^{h\nu/kT(r)} - 1}\ \mathrm{erg\,s^{-1}\,\AA^{-1}}, \tag{4}$$

where $T(r) = 2.2 \times 10^5 \dot{M}_{26}^{1/4} M_8^{1/4} r_{14}^{-3/4}$ K, i is the angle between the disk normal and the LOS ($\sim 82^\circ$ in NGC 4258), $\dot{M}_{26}$ is the accretion rate in units of $10^{26}\,\mathrm{g\,s^{-1}}$, M_8 is the central mass in units of $10^8\,\mathrm{M_\odot}$, and r_{14} is the radius in units of 10^{14} cm. For $\dot{M}/\alpha = 10^{-1.7}\,\mathrm{M_\odot\,yr^{-1}}$ and $r_{out} = 4 \times 10^4\,\mathrm{R}_S$, equation 4 indicates that $L_{5500}^{(td)} \lesssim 10^{37}\,\mathrm{erg\,s^{-1}\,\AA^{-1}}$ for $r_{tr} \gtrsim 10^2\,\mathrm{R}_S$. *At the accretion rates required by the ADAF models, the outer thin disk must extend to within* $\sim 10^2\,R_S$ *in order to generate sufficient optical luminosity. This is additional, independent evidence that* $r_{tr} \lesssim 10^2\,R_S$ *in NGC 4258.*

The masers in NGC 4258 extend from 0.13 pc to 0.26 pc, and the cause of the observed inner edge at $4 \times 10^4\,\mathrm{R}_S$ is uncertain. The present observations effectively disqualify one of the most promising theories: that the inner edge of the masing zone corresponds to r_{tr} and to the inner edge of the outer cool disk itself. Even if NGC 4258 is powered by an ADAF, the lack of 22-GHz emission requires that the outer thin disk extends to well within $4 \times 10^4\,\mathrm{R}_S$, and another explanation is needed to account for the lack of masers in this region. We note that Neufeld & Maloney (1995) argue that a proposed flattening of the disk at small radii would reduce the disk's exposure to central, hard X-rays, and may account for the lack of maser emission within 0.13 pc.

There are a great many low-luminosity accreting systems, encompassing a wide variety of types and spanning many decades in central mass, that are apparently sufficiently sub-Eddington to be plausible ADAF candidates. However, for most of these systems, a standard Shakura-Sunyaev thin disk is also a viable solution. Thus, while there is compelling evidence for the existence of ADAFs in some systems, it remains unclear to what extent the optically thin, two-temperature ADAF is in general applicable. Unfortunately, a physically motivated explanation for how ADAFs are triggered in the first place remains elusive, and, until this 'on-switch' is discovered, questions concerning the universality of ADAFs must necessarily be addressed empirically. NGC 4258 is a useful place to explore this issue, since it is highly sub-Eddington, and because the nuclear maser and VLBI together provide access to a host of usually obscure parameters. While the present 22-GHz non-detection does not rule out the presence of an ADAF in NGC 4258, it does begin to place interesting constraints on the geometry of any proposed ADAF.

We thank R. Mahadevan and R. Narayan for helpful discussions, and C. Henkel for valuable assistance in conducting the observations at Effelsberg.

REFERENCES

Blandford, R. D. & Königl, A. 1979, *ApJ*, 232, 34

Cecil, G., Wilson, A. S., & Tully, R. B. 1992, *ApJ*, 390, 365

Claussen, M. J., Heiligman, G. M., & Lo, K. Y. 1984, *Nature*, 310, 298

Esin, A., McClintock, J. E., & Narayan, R. 1997, *ApJ*, in press (astro–ph/9705237)

Frank, J., King, A., & Raine, D. 1992, *Accretion Power in Astrophysics, 2nd ed.*, Cambridge University Press

Greenhill, L. G., Jiang, R. D., Moran, J. M., Reid, M. J., Lo, K. Y., & Claussen, M. J. 1995, *ApJ*, 440, 619

Herrnstein, J. R., PhD Dissertation, Harvard University, 1997

Herrnstein, J. R. , Moran, J. M., Greenhill, L. J., Diamond, P. J., Miyoshi, M., Nakai, N., & Inoue, M. 1997, *ApJ*, 475, L17

Herrnstein, J. R., Greenhill, L. J., & Moran, J. M. 1996, *ApJ*, 468, L17

Lasota, J.-P., Abramowicz, M. A., Chen, X., Krolik, J., Narayan, R., & Yi, I. 1996, *ApJ*, 462, 142 (L96)

Mahadevan, R. 1997, *Ap. J.*, 477, 585 (M97)

Mahadevan, R. & Quataert, E. 1997, *Ap. J.*, 490, in press (Astro–ph/9705067)

Makishima, K., Fujimoto, R, Ishisaki, Y., Kii, T., Lowenstein, M., Mushotzky, R., Serlemitsos, P., Sonobe, T., Tashiro, M., & Yaqoob, T. 1994, *Proc. Astron. Soc. Jpn.*, 46, L77

Manmoto, T., Mineshige, S., & Kusunose, M. 1998, *ApJ*, in press

Miyoshi, M., Moran, J. M., Herrnstein, J. R., Greenhill, L. J., Nakai, N., Diamond, P. J., & Inoue, M. 1995, *Nature*, 373, 127

Moran, J. M., Greenhill, L. J., Herrnstein, J. R., Diamond, P. J., Miyoshi, M., Nakai, N., & Inoue, M. 1995, *Proc. Natl. Acad. Sci. USA*, 92, 11427

Mushotzky, R. F., Done, C., & Pounds, K. A. 1993, *ARA&A*, 31, 717

Nakai, N., Inoue, M., & Miyoshi, M. 1993, *Nature*, 361, 45

Narayan, R. 1997, in *Accretion Phenomena and Related Outflows*, eds. D. Wickramasinghe, G. Bicknell, & L. Ferrario, 75

Narayan, R. & Yi, I. 1994, *ApJ*, 428, L13

Narayan, R. & Yi, I. 1995a, *ApJ*, 444, 231

Narayan, R. & Yi, I. 1995b, *ApJ*, 452, 710 (NY95b)

Narayan, R., Yi, I., & Mahadevan, R. 1995, *Nature*, 374, 623

Narayan, R., Mahadevan, R., Grindlay, J. E., Popham, R. G., & Gammie, C. 1998, *ApJ*, 492, 554.

Neufeld, D. A. & Maloney, P. R. 1995, *ApJ*, 447, L17

Shakura, N. I. & Sunyaev, R. A. 1973, *A&A*, 24, 337

Watson, W. D. & Wallin, B. K. 1994, *ApJ*, 432, L35

Wilkes, B. J., Schmidt, G. D., Smith, P. S., Mathur, S., & McLeod, K. K. 1995, *ApJ*, 455, L13